ACS chemical biology

Articles

pubs.acs.org/acschemicalbiology

Identification of Small Molecule Modulators of Gene Transcription with Anticancer Activity

Tram Anh Tran,[†,+] Jennifer Wichterman-Kouznetsova,[‡,+] Diana Varghese,[†] Ruili Huang,[‡] Wenwei Huang,[‡] Matthias Becker,[§,#] Christopher P. Austin,[‡] James Inglese,[‡] Ronald L. Johnson,[‡,⊥] and Elisabeth D. Martinez*[,†,∥]

[†]Hamon Center for Therapeutic Oncology Research and [∥]Department of Pharmacology, University of Texas Southwestern Medical Center, Dallas, Texas 75390, United States

[‡]NIH Chemical Genomics Center, NCATS, NIH, Rockville, Maryland 20850, United States

[§]Laboratory of Receptor Biology and Gene Expression, NCI, NIH, Bethesda, Maryland 20892, United States

Supporting Information

ABSTRACT: Epigenetic regulation of gene expression is essential in many biological processes, and its deregulation contributes to pathology including tumor formation. We used an image-based cell assay that measures the induction of a silenced GFP-estrogen receptor reporter to identify novel classes of small molecules involved in the regulation of gene expression. Using this Locus Derepression assay, we queried 283,122 compounds by quantitative high-throughput screening evaluating compounds at multiple concentrations. After confirmation and independent validation, the Locus Derepression assay identified 19 small molecules as new actives that induce the GFP message over 2-fold. Viability assays demonstrated that 17 of these actives have anti-proliferative activity, and two of them show selectivity for cancer versus patient-matched normal cells and cause unique changes in gene expression patterns in cancer cells by altering histone marks. Hence, these compounds represent chemical tools for understanding the molecular mechanisms of epigenetic control of transcription and for modulating cell growth pathways.

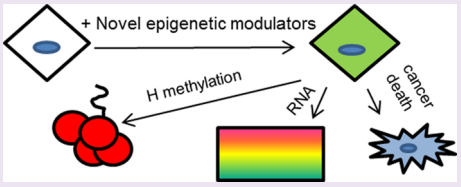

Classical epigenetic targets such as histone deacetylases (HDACs) and DNA methyltransferases (DNMTs) have been chemically targeted over the past decade in preclinical cancer models, and more recently a few have advanced to clinical trials for proliferative diseases and gained FDA approval.[1−8] Besides histone deacetylation or DNA methylation, chemical modulation of other enzymatic activities such as histone methylation or demethylation represent additional targets for chemical intervention in various clinical settings. Efforts in this area have yielded, over the past few years, a number of compounds of interest that target histone methyltransferases, histone demethylases, or bromodomain proteins,[9−15] among others. The challenge in some cases has been obtaining cellular activity from inhibitors developed *in vitro*.

To identify small molecules involved in regulation of transcription, we utilized a cell-based imaging assay that monitors the induction of a silenced GFP reporter gene. This assay, termed Locus Derepression (LDR), is based on a GFP reporter gene under the control of the cytomegalovirus (CMV) promoter stably integrated in the genome of C127 mouse mammary adenocarcinoma cells.[16] Although typically constitutively active, the CMV promoter that drives GFP expression in LDR cells is transcriptionally silenced. Small molecules, like histone deacetylase (HDAC) or DNA methyltransferase (DNMT) inhibitors, activate transcription of the reporter, suggesting the locus is under some level of epigenetic repression.[16] Induction of GFP production in LDR cells can be assayed using a laser scanning microplate cytometer in a format suitable for high-throughput screening. Miniaturization of this assay in 1536-well plate format[17] enabled an initial quantitative high-throughput screen (qHTS) of over 70,000 small molecules tested at seven different concentrations, which identified structurally unique compounds showing anticancer activity,[18] including the 8-hydroxyquinoline chemotype subsequently also identified and developed by others.[15] To expand our efforts, we have now undertaken a rescreen using a larger library of over 280,000 compounds. The rescreen identified new active series and confirmed a subset of originally observed active compounds. Here, we describe the screening, validation, and characterization strategies that led to the identification of 19 new bona fide small molecule transcriptional modulators with biological activity, 17 of which inhibit cell viability and 2 of which are selective for cancer versus normal cells. These compounds are now available as probes for further elucidation of their epigenetic and transcriptional effects as well as their anti-proliferative activities.

Received: December 19, 2013
Accepted: September 4, 2014
Published: September 4, 2014

RESULTS AND DISCUSSION

Characterization of the LDR Assay. Since the LDR assay is responsive to DNMT inhibitors and HDAC inhibitors,[16,19] we evaluated if the CMV promoter driving GFP in our system harbored the corresponding epigenetic marks. Bisulfite sequencing confirmed DNA methylation of CpG sites within the CpG island of the CMV promoter (Figure 1A and Supplementary Figure 1), which likely contributes to gene silencing since the active CMV promoter typically is not DNA methylated.[20,21] In addition, chromatin immunoprecipitation assays demonstrated that the promoter has a low basal level of histone acetylation, which markedly increases upon treatment of the cells with trichostatin A (Figure 1B), further validating the use of this system for screening efforts to identify epigenetic modulators.

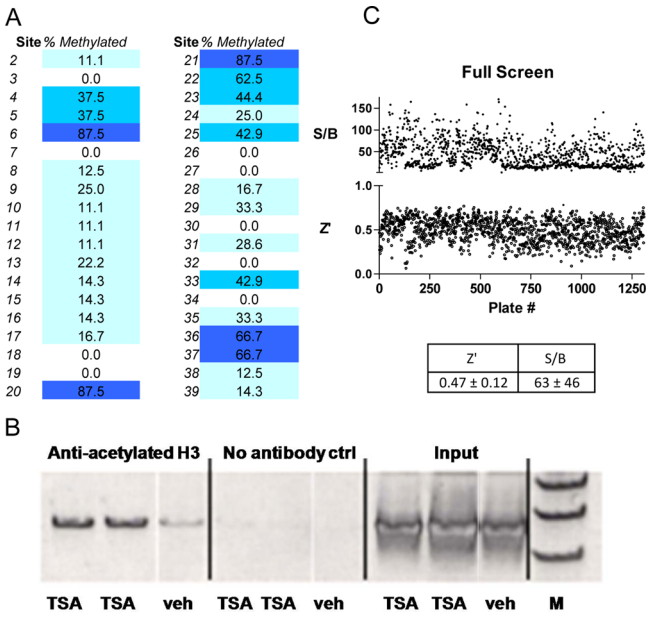

Figure 1. Features of the LDR assay. (A) Bifulfite sequencing of LDR cells shows constitutive DNA methylation in approximately one-third of the CpG dinucleotides present in the CMV promoter. The percent of colonies that showed methylation at each site is denoted, and the level of methylation is represented by shades of blue (dark blue = highest methylation). (B) TSA increases histone 3 acetylation at the CMV promoter. Nuclei from LDR cells treated with DMSO vehicle or TSA (250 ng/mL) for 24 h were used in chromatin immunoprecipitation assays to measure the levels of acetylated H3 associated with the CMV promoter. No antibody lanes are background signal and represent samples that underwent the ChIP procedure but without antibody present. Input lanes show signal derived from 10% starting material prior to ChIP. White vertical slivers mark areas where unrelated gel lanes were deleted from the blot for clarity of presentation. M represents the molecular weight marker. (C) Assay performance. The Z′ scores and signal to background ratios (S/B) for the full LDR screen covering over 1250 plates are shown. The average Z′ scores and S/B ratios are given in the table along with standard deviations.

Quantitative High-Throughput Screen of the LDR Assay. The LDR qHTS (Supplementary Table 1) was conducted using an integrated robotic platform[22] and comprised 1309 1536-well plates. The LDR assay was screened against 283,122 small molecule samples (described in the Methods section) arrayed as a six-point interplate concentration series and screened from the lowest (3 nM) to the highest (50 μM) concentration. The assay performance was stable throughout the screen, as indicated by a mean signal to background ratio of 63 and a mean Z′ score of 0.47 (Figure 1C). A titration of sodium butyrate, a positive control compound present on every assay plate, performed consistently throughout the screen showing 4 ± 1.7 mM mean half-maximal excitation concentration (EC_{50}), a value that was similar to previous determinations.

Following the qHTS, the concentration−response data for each sample was fitted using a custom algorithm,[23] and the resulting curves were classified by efficacy and goodness of fit measures.[24] Briefly, well fit ($r^2 \geq 0.9$) curves displaying two asymptotes were denoted Class 1, while those having a single asymptote were denoted Class 2. Both classes were subdivided by percent efficacy where Class 1.1 and 2.1 curves had efficacy greater than 80% and Class 1.2 and 2.2 curves showed efficacy between 30% and 80%. Curves displaying a poor fit ($r^2 < 0.9$) or activity at only the highest concentration were designated Class 3. Concentration−response data showing curve fits with <30% efficacy or lacking a significant curve fit were denoted Class 4 and considered inactive.

The qHTS identified 5,462 samples representing 2% of the library as positive (Classes 1−3) in the LDR assay (Table 1).

Table 1. Potency and Curve Categories of LDR Actives

	curve class					
EC_{50} (μM)	1.1	1.2	2.1	2.2	3	total
<1	16	15	0	8	109	148
1−10	121	95	63	130	684	1093
>10	0	0	240	270	3711	4221
total	137	110	303	408	4504	5462
% library	0.05	0.04	0.11	0.14	1.6	1.9

About 10% (550) of these positives were considered good quality curves (Classes 1.1, 1.2, and 2.1) showing a range of potencies, with 31 positives having EC_{50} values of <1 μM. Approximately 5% (279) of the qHTS actives had 1−10 μM EC_{50} values, and another 5% (240) had EC_{50} values of >10 μM. The remainder of the positives had lower quality curves (Classes 2.2 and 3) for which the EC_{50} determinations were considered inconclusive. The majority of these samples showed activity only above 10 μM.

Identification of Active Series. To identify structurally related series, 680 LDR positives (all samples with Class 1.1, 1.2, and 2.1 curves, as well as Class 2.2 curves with >50% efficacy) were clustered using a custom scaffold detection program. This process yielded 139 singletons and 663 structural series containing at least three compounds with one or more actives. Because an active could be part of more than one series, the number of series and singletons was larger than the number of samples clustered. After clustering, structurally related compounds with inconclusive or no activity were added to each series.

The 663 series and 139 singletons were then annotated for potential liabilities. Of this set, 80 series and 5 singletons had no liabilities. Eleven series were scored as fluorescent because they were active for solution fluorescence or identified as fluorescent in other internal GFP screens.[25] Singletons with potency >5 μM or <50% efficacy as well as series containing significantly fewer numbers of actives compared to the mean of all LDR series were deprioritized. After excluding compounds and series with poor chemical tractability, 201 compounds

dx.doi.org/10.1021/cb500532x | ACS Chem. Biol. 2014, 9, 2603−2611

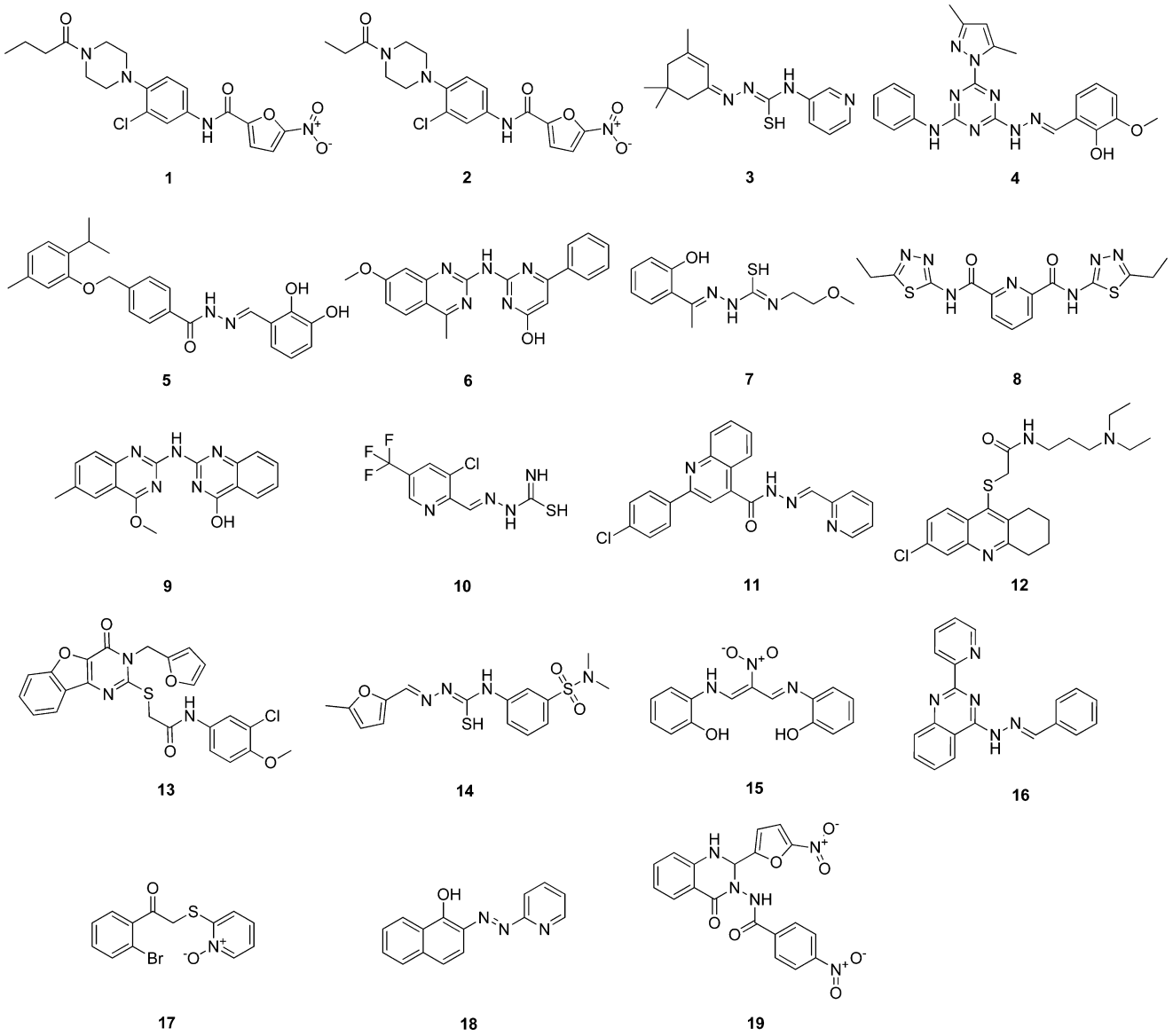

Figure 2. Structures of small molecule actives that induce the LDR-GFP transcript. The structures of hit compounds that passed validation and retest and showed induction of the GFP transcript in LDR cells are shown. Information on their potency and biological activity can be found in tables throughout this manuscript.

representing 130 series and 47 singletons were selected. An additional 27 compounds were added, which had been excluded from the clustering analysis (Class 2.2 with <50% efficacy) but had <5 μM EC_{50}.

These retest compounds were titrated and tested in the imaging assay using parental or LDR cells, with both lines tested twice in two independent experiments. The parental cells, which lack the GFP transgene, were used to identify fluorescent compounds that emit light in the same range as GFP. The parental cell assay identified 87 of the 228 compounds (38%) as active in one or both experiments, indicating that these were likely fluorescent artifacts (data not shown). In the LDR retest assay, 72 nonfluorescent compounds were scored as positive in one or two runs (Supplementary Table 2).

For confirmation, 55 active and 5 inactive retest compounds were chosen for testing as independent samples, and in this confirmation 90% of originally active compounds were reconfirmed as active (Supplementary Table 3). Ten retest actives were not chosen for independent confirmation because they were either known bioactives or structurally related to chosen actives or were previously identified LDR actives.[18] Of these 60 unique compounds, the parental cell imaging assay identified 23 independent samples as potentially fluorescent, and these were excluded from further followup. Of the remaining 37 nonfluorescent compounds, the LDR assay recovered 19 as active (positive in both runs), 10 as inconclusive (positive in one run only), and 8 as inactive (Supplementary Table 3).

Characterization of Confirmed Positives. To test if the confirmed positive compounds in the LDR assay increased GFP levels by inducing its transcription, GFP transcript levels were measured by qRT-PCR. All compounds that scored as active or inconclusive in the confirmation LDR assay as well as some inconclusive fluorescent compounds were tested. Each compound was incubated with LDR cells at a concentration above its determined EC_{50} value (Supplementary Table 3) for 24 h. Total RNA was then extracted from cells, and GFP

dx.doi.org/10.1021/cb500532x | ACS Chem. Biol. 2014, 9, 2603−2611

transcript levels were determined by qRT-PCR with mTBP as the reference gene (using cyclophilin as the reference gave equivalent results; data not shown). Relative to DMSO-treated cells, 200 nM Trichostatin A, a known activator of the LDR GFP reporter,[19] induced GFP transcripts by at least 5-fold, while 19 positives (14 actives and 5 inconclusives) induced GFP transcription by 2-fold or greater. Figure 2 shows the structures of these 19 positives, and Table 2 shows the GFP

Table 2. Confirmed LDR Actives by GFP Protein and mRNA Expression

		LDR activity[a] (microscopy)		mRNA GFP induction[a] (qRT-PCR)	
compd	sample ID	EC_{50} (μM)	% efficacy	fold	dose (μM)
1	MLS000718916-01	1	22	11	10
2	MLS000718915-01	2	38	20	10
3	MLS001033723-01	3	95	152	10
4	MLS000541035-01	4	104	8	10
5	MLS000408882-01	4	23	59	10
6	MLS000777862-01	6	100	12	10
7	MLS000417681-01	7	98	3	25
8	MLS000079004-01	8	96	7	25
9	MLS000112490-01	8	39	4	25
10	MLS001111252-01	8	42	26	25
11	MLS000699226-01	10	61	102	25
12	NCGC00110901-01	10	63	38	25
13	NCGC00112814-01	13	37	21	25
14	MLS000776252-01	14	34	3	25
15	MLS000777314-01	18	29	12	50
16	MLS000769838-01	20	97	4	50
17	MLS001033348-01	28	127	218	50
18	MLS000573813-01	32	75	8	50
19	MLS000727703-01	32	27	3	50

[a]EC_{50} values and fold induction values are for overnight treatments.

induction measured by qRT-PCR. Several compounds induced GFP expression greater than 100-fold while not altering the expression of the reference genes (Table 2 and Supplementary Table 4), demonstrating a selective potent induction of the silent transgene.

To determine whether the confirmed compounds that induced GFP mRNA expression showed anticancer activity, we screened them first for inhibition of viability against the LDR cells using standard MTS assays. Out of the 19 compounds, 17 were effective in blocking the proliferation of LDR cells with IC_{50} values ranging from 0.8 to 49 μM (Table 3 and Figure 3a). Twelve of these had good potency, showing IC_{50} values of <4 μM. To determine if these compounds exhibited selectivity for cancer versus normal cells, we measured viability of the non-small cell lung cancer line HCC4017 and the patient-matched normal human bronchial epithelial line HBEC30KT[18] in response to treatment with the confirmed actives. Compounds **5** (MLS000408882) and **18** (MLS000573813) showed specificity for cancer versus normal cells (Table 3). This was demonstrated by the greater than 6-fold shift in sensitivity to compound **5** in the cancer versus the normal cells (IC_{50} of 1.3 μM for HCC41017 versus 8.1 μM for HBEC30KT cells). Similarly, there was a 2-fold shift in IC_{50} for compound **18** (IC_{50} of 6.5 μM for HCC41017 versus 13 μM for HBEC30KT cells) as shown in Figure 3B and Table 3.

Table 3. Cell Viability in Response to Active Compounds after 4 Days of Treatment[a]

compd	LDR IC_{50} value (μM)	SD	HBEC30KT IC_{50} value (μM)	SD	HCC4017 IC_{50} value (μM)	SD
1	1.0	0.5	3		8	
2	1.4	1.2	25		47	
3	2.5	1.2	>50		>50	
4	1.0	0.2	3.8	1.4	6.6	3.6
5	**1.5**	**0.3**	**8.1**	**0.6**	**1.3**	**0.5**
6	2.4	1.1	2		4.5	
7	3.6	1.6	>50		>50	
8	3.6	2.1	>50		>50	
9	1.2	0.3	8		16	
10	12.0	1.4	14	10	10	1
11	>50		>50		>50	
12	43.5	5	>50		>50	
13	>50		>50		>50	
14	21.5	13.4	50		40	
15	44	8.5	13		10	
16	1.2	0.3	1.6	0.07	1.35	0.07
17	2.2	0.2	48		33.5	3.5
18	**0.8**	**0.1**	**13**	**2**	**6.5**	**2**
19	49	1.4	>50		>50	

[a]Data for compounds **5** and **18**, which are cancer-selective, are shown in bold.

Treatment with compounds **5** and **18** led to decreased cell numbers and increased cell death as demonstrated by Annexin V staining (Figure 3C and D), consistent with the observed lower viability.

To investigate the transcriptional changes induced by these compounds that may contribute to their selective anticancer effects and to evaluate the mode of action of compound **5** versus **18**, we performed global gene expression profiling in the patient-matched cell line pair after 4 h and after 24 h of treatment (Supplementary Data 1). These studies yielded unique cancer-specific gene expression signatures for compounds **5** and **18**. About 250 genes were upregulated 3-fold or more, and 270 were downregulated at least 3-fold within 4 h by compound **5** in the cancer line. Of these, only 4 genes were upregulated 3-fold or greater, and 3 genes were downregulated 3-fold or more in the normal cells. Similarly, most of the genes altered in the normal HBEC30KT cells were not modulated by compound **5** in the cancer HCC4017 patient-matched line. Clearly then, compound **5** reprograms transcriptional patterns in a unique manner in cancer versus normal cells. An analogous pattern was observed with compound **18**. After 4 h, 311 genes were upregulated 3-fold or more and 340 were downregulated in the cancer cells, while of these only 12 were upregulated and 4 downregulated by 3-fold or more in the normal line, again indicating a distinct transcriptional response. To validate common as well as compound-specific genes selectively modulated in cancer, we performed qRT-PCR on a subset of the genes differentially modulated in the HCC4017/HBEC30KT cell line pair. This indeed confirmed that compounds **5** and **18** partly normalize transcriptional patterns in cancer (Figure 4A–D and Supplementary Figure 2). These data suggest that compound-induced cancer-specific transcriptional changes may contribute to the selective anticancer phenotype of these small molecules. If so, transcriptional changes should be expected at doses at or below the IC_{50} for inhibition of cell viability. Indeed, we observed strong induction

dx.doi.org/10.1021/cb500532x | ACS Chem. Biol. 2014, 9, 2603–2611

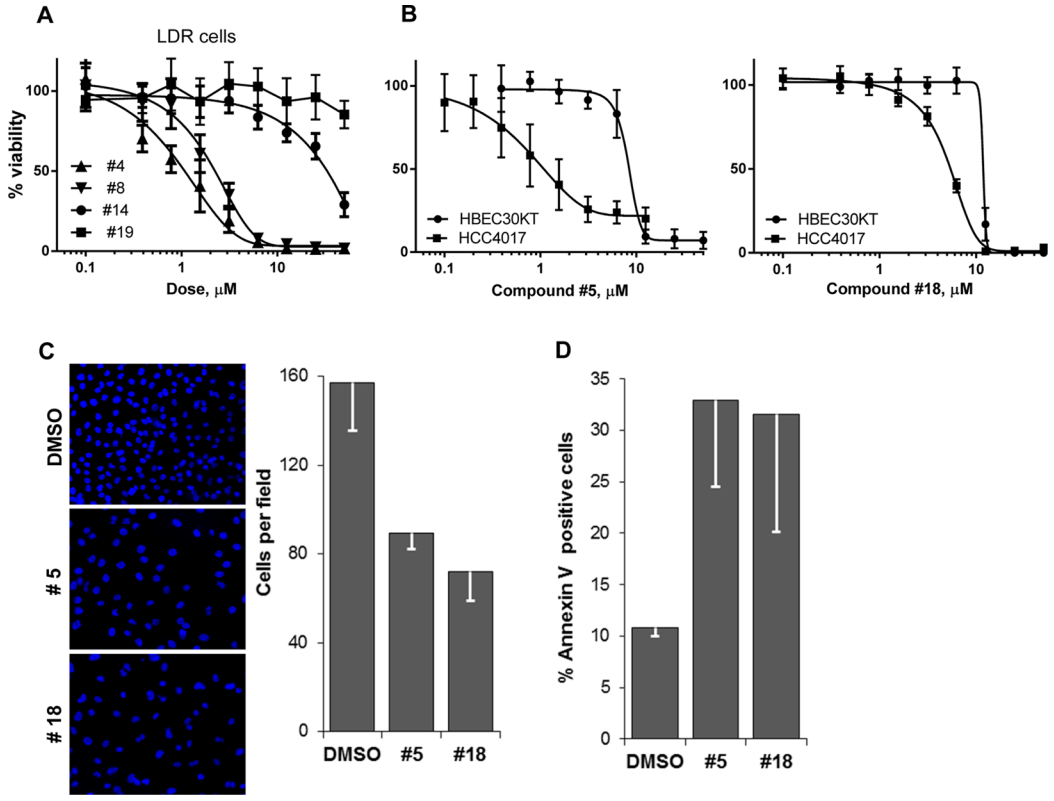

Figure 3. Anti-proliferative potency and selectivity of select confirmed actives. (A) Shown are fractions of viable LDR cells after 4 days of treatment with a subset of confirmed actives with different potencies (classified as potent (**4**, **8**), intermediate (**14**), and ineffective (**19**)). (B) Cell lines derived from a human non-small cell lung tumor (HCC4017) or patient-matched normal bronchial epithelial tissue (HBEC30KT) were treated with compound **5** or **18** at the indicated concentrations for 4 days, and viability was determined by standard MTS assays. (C and D) Cells were plated at 4700 cells/cm^2 for 24 h (C) or 48 h (D), treated with indicated compound (**5**, 1.3 μM and **18**, 6.5 μM) for 48 h (C) or 72 h (D), and then harvested for cell number (C) or FACS analysis (D). (C) Analysis of cell number by DAPI staining. Left, fluorescence images taken at 200× magnification; right, quantification of cells per field of images on the left. Data are averages from 7 images for each treatment condition; error bars represent SEM. (D) Percentage of Annexin V positive cells was determined by FACS. Data are averages from two independent experiments with error bars representing SEM.

of gene expression at compound **5** doses at or below the IC_{50} for LDR cells, while TSA induced GFP expression less robustly and only at doses above its IC_{50} (Supplementary Figure 3A). This phenotype was even more striking in the matched pair where compound **5**, but not TSA or 5-azadeoxycytidine, upregulated the expression of a cancer downregulated gene (ANGPTL4) at doses below, at, and above its IC_{50} (Supplementary Figure 3B) and restored the expression of a gene transcribed in normal cells but not constitutively expressed in the matched cancer line (Supplementary Figure 4). This suggests that compound **5** modulates transcription by mechanisms distinct from histone acetylation and/or DNA methylation.

To determine if compound **5** was modulating transcription by altering histone marks, we first measured global histone modifications by Western blot analysis. In independent experiments, we observed no changes in histone acetylation in response to treatment with compound **5** but clear increases in histone methylation at both activating and repressive marks (Figure 5A). Changes in histone methylation could also be seen by ChIP experiments measuring the activating H3K4me3 mark on the promoter of the strongly induced endogenous ANGPTL4 gene. Indeed, histone methylation levels were increased near the transcription start site, indicating regulation of ANGPTL4 at the chromatin level in response to compound **5** (Figure 5B). Together, these studies suggest that compound **5** targets cancer-selective susceptibilities at the epigenetic/transcriptional level and that its anti-proliferative action may involve the reversal of cancer-specific gene expression patterns through modulation of histone methylation.

Conclusions. By using a cell-based assay designed to find small molecules with the ability to reactivate an epigenetically silenced locus and turn on its transcription, we have identified 19 validated novel potential transcriptional modulators. These compounds increase expression of the silenced transgene ranging from modest 2-fold to more than 100-fold. This ability to modulate transcription, perhaps combined with other compound activities, results in anticancer properties as exhibited for 17 out of the 19 small molecules. The variety in anticancer activity and potency of these compounds suggests potential mechanistic diversity in this set of small molecules, in addition to the existing structural diversity. The finding that two compounds (**5** and **18**) show selectivity for cancer versus normal cells with higher potency in specifically killing cancer cells further validates the diversity in mode of action captured by the assay actives. Furthermore, even these two compounds were partly distinct in the genes they altered transcriptionally, again pointing to mechanistic diversity. The 19 small molecules reported here do not exhibit structural similarities to compounds of known mode of action and thus constitute novel probes.

dx.doi.org/10.1021/cb500532x | *ACS Chem. Biol.* 2014, 9, 2603−2611

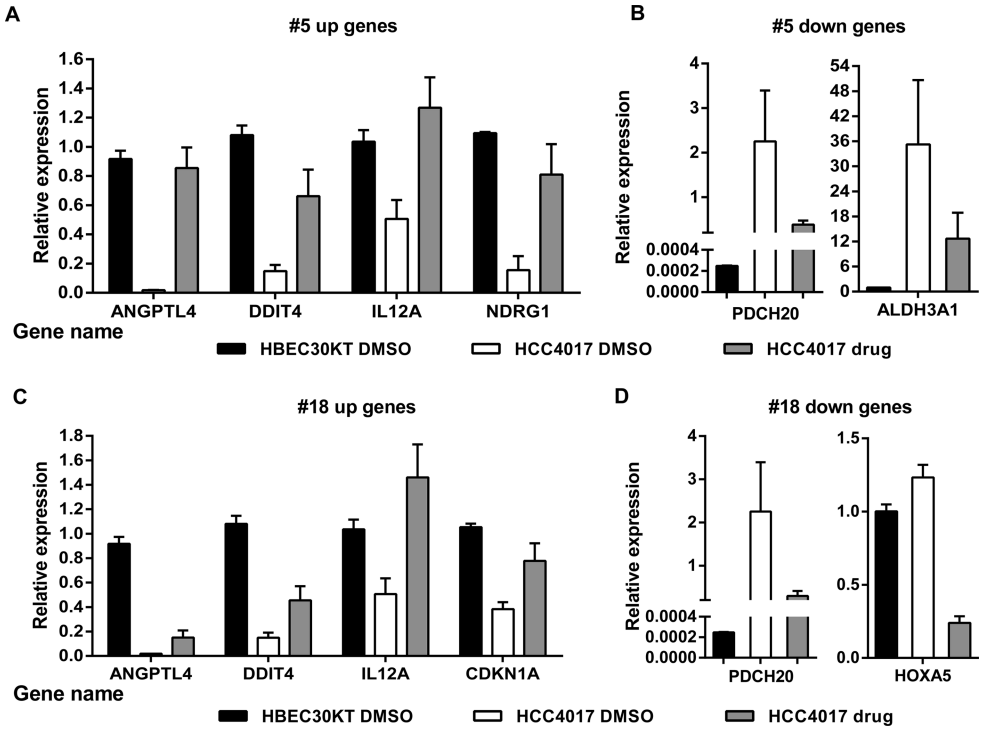

Figure 4. Compounds **5** and **18** normalize transcriptional patterns. (A–D) Confirmation of microarray data by qRT-PCR confirming changes observed in the microarray data after 4 h treatments (1.3 μM for compound **5**; 6.5 μM for compound **18**). Shown are examples of genes upregulated by compound **5** (A) or compound **18** (C) in a cancer-specific manner or downregulated by treatment (B, D). The changes of some genes are common between the two compounds, while others are unique (NDRG1 and ALDH3A1 change upon compound **5** treatment, whereas compound **18** treatment changes expression of CDNK1A and HOXA5). Expression was normalized to TBP and expressed relative to HBECT30KT treated with DMSO. Data is average + SEM of two independent experiments.

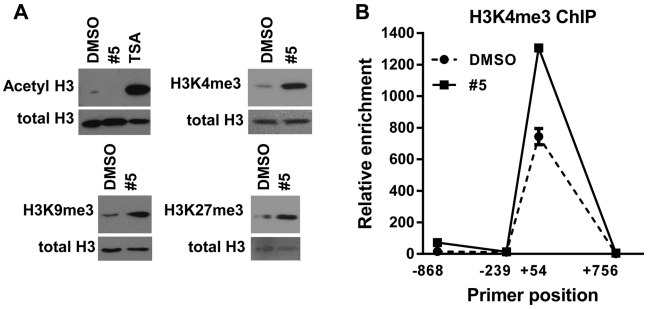

Figure 5. Compound **5** modulates histone methylation in cells. (A) Western blot analysis of histone extracts from LDR cells treated with indicated compounds at IC_{50} doses (**5**, 1.5 μM; TSA, 14 nM) for 24 h. (B) H3K4me3 ChIP analysis of the ANGPTL4 promoter upon treatment of HCC4017 cancer cells with compound **5** (1.3 μM for 24 h). Data is average ± SEM from two independent experiments.

Our previous screening efforts identified chemical probes with transcriptional and epigenetic modulatory activity.[18,19] Among these, several have been further developed by ourselves or others and have been found to have anti-proliferative properties and to function through the inhibition of novel epigenetic molecular targets, including histone demethylases of the Jumonji family.[15,26] The active compounds identified in the present study may likewise develop into chemical tools to pharmacologically modulate epigenetic enzymes or probe new aspects of transcriptional programs. The cancer selectivity of compounds **5** and **18** implies that the cellular targets of these small molecules may indeed exert cancer specific functions or constitute a cancer-specific susceptibility. Of particular interest are the distinct transcriptional profiles that each of these two compounds elicits in cancer versus normal cells. Although we have no direct evidence that these changes may trigger the selective anticancer activity observed, it can be speculated that they contribute to this phenotype.

Among recently identified epigenetic modulators of known function, inhibitors of histone demethylases, of histone methyltransferases, and of bromodomain proteins have shown some degree of anticancer activity.[10,26−29] In addition, some of these compounds[11] have also demonstrated effectiveness in cellular models of other human diseases including inflammation, suggesting that the therapeutic potential is broad. The structures we have uncovered in this study, by virtue of their similarity and novelty to currently described chemotypes, attests to the utility of cell-based assay strategies for the identification of epigenetic modulators. Our data strongly demonstrates, for example, the involvement of histone methylation in the mode of action of compound **5**. Further investigation beyond the scope of the present study should lead to the identification of the cellular targets (likely histone methylases or demethylases) of this highly interesting compound. While the ability to identify specific targets and define mechanisms of action for all of these small molecules remains a challenge, improved methods and reagents are continually evolving[30,31] to address this aspect of phenotypic screening.

METHODS

Cell Culture. C127 parental cells (kindly provided by Dr. Gordon Hager) and Locus Derepression (LDR) cells[32] were cultured in Dulbecco's Modified Eagle's medium (DMEM) with 0.58 g/L L-

dx.doi.org/10.1021/cb500532x | ACS Chem. Biol. 2014, 9, 2603−2611

glutamine and 4.5 g/L glucose, supplemented with 1 mM sodium pyruvate, 0.1 mM minimal essential medium (MEM) nonessential amino acids, 1% (v/v) penicillin-streptomycin, and 10% heat-inactivated fetal bovine serum (FBS). Lung cancer cell line HCC4017 (provided by Dr. J. D. Minna) was maintained in RPMI 1640 media supplemented with 5% FBS. Immortalized normal human bronchial epithelial cells (HBEC30KT) provided by Dr. J. D. Minna were cultured in keratinocyte serum-free medium supplemented with pituitary extract and epidermal growth factor (Invitrogen) as previously described.[33]

Bisulfite Sequencing and Chromatin Immunoprecipitation in LDR Cells. For bisulfate sequencing, genomic DNA from LDR assay cells treated as indicated was isolated and bisulfite treated. After purification, this DNA was used as template for PCR amplification using CMV specific primers, and PCR products were subcloned and introduced into bacteria using the TOPO TA cloning kit. White colonies were grown, and plasmid DNA was isolated for sequencing. Percent methylation was indicated for each CpG site from an average of about 10 colonies. For chromatin immunoprecipitation, LDR cells were treated overnight with 250 ng/mL of trichostatin A or vehicle, harvested, and treated with formaldehyde to cross-link DNA and proteins. Chromatin immunoprecipitations were carried out following standard protocols with an anti-acetylated histone 3 antibody (Millipore-Upstate). After cross-link reversal, PCR was performed using primers specific to the CMV promoter.

Quantitative High-Throughput Screen. The LDR screen was performed on an integrated robotic platform as previously described.[17,18] For the detailed protocol, see Supplementary Table 1. Briefly, cells were harvested, passed through a 40-μm filter, and suspended at 50,000 cells per mL in growth medium. Cells were seeded at 250 cells/5 μL/well into black, clear-bottom, 1536-well assay plates (Aurora Discovery) using a Multi-Drop Combi (Thermo Scientific). Compounds and controls (23 nL) were transferred via Kalypsys pin tool to each well of the assay plate, resulting in a 217-fold dilution. Following a 30-h incubation at 37 °C and 5% CO_2, the plates were washed twice with 6 μL of phosphate-buffered saline (PBS). GFP expression was detected by a laser scanning microplate cytometer,[34] Acumen Explorer (TTP LabTech), with the following settings: 6 mW and 488 nm laser, 660 V 500−530 nm photomultiplier tube, 1 × 8 μm x and y scan resolution, 2.4 standard deviations above the background trigger threshold, and 15 μm minimum and 120 μm maximum feature size.

Chemicals. Please refer to Supporting Information for detailed description of chemicals.

Data Analysis. Analysis of compound concentration−response data was performed as previously described.[24,35] Please refer to Supporting Information for a detailed description of data analysis.

qRT-PCR Analysis. Exponentially growing LDR, HCC4017, or HBEC30KT cells were plated in 10 cm dishes and treated the next day for 4 or 24 h with the indicated compounds at doses shown in Table 2 for LDR cells or in the legend to Figure 4 for the matched pair lines, or with TSA or vehicle controls. Cells were harvested and processed for RNA extraction (RNeasy kit, Qiagen). The extracted RNA was quantified, DNase treated, and reverse transcribed. The resulting cDNA was amplified in SYBR green real-time quantitative PCR assays (Applied Biosystems) with validated primers specific for each gene of interest, as shown in Supplementary Table 5. Reactions were performed on an ABI Prism 7900HT with an initial 2 min preincubation at 50 °C, followed by 10 min at 95 °C and then 40 cycles of 95 °C for 15 s and 60 °C for 1 min. mTBP for LDR cells or hTBP for matched pair cells was used as the reference gene. The ΔΔCt method was used to analyze the data.[36] Expression levels were calculated as fold over DMSO as indicated in individual legends. Reactions were run in triplicate. All primers are described in Supporting Information.

MTS Viability Assays. LDR cells (750 cells/well) or the matched lung cancer cell line pair HCC4017 (1500 cells/well) and HBEC30KT (2500 cells/well) were plated on 96-well dishes and grown overnight at 37 °C, 5% CO_2 before being treated with increasing doses of investigational compounds with maximal concentrations as shown in Table 2. Four days later viability was measured using the Cell Titer 96 Aqueous One kit (Promega). Absorbance at 490 nm (with 650 nm as reference) was measured on an Omega Plate reader (BMG LabTech). Data were normalized to untreated cells set at 100% viability. Each cell line was tested in 2−5 independent experiments each containing 4−8 replicates. Dose−response curves were plotted using a nonlinear regression model, and IC_{50}'s were determined from the fitted curves.

Determination of Cell Numbers. HCC4017 cells were plated at 4700 cells/cm^2 on glass coverslips. The next day, cells were treated with vehicle, 1.3 μM compound **5** or 6.5 μM compound **18** for 48 h, then fixed, permeabilized, and stained with DAPI. Images of random fields were taken using a Nikon Eclipse 80*i* fluorescence microscope at 200× magnification. Number of cells per field was determined using ImageJ software (http://imagej.nih.gov/ij).

Analysis of Cell Death. HCC4017 cells were plated as indicated above in 60 mm dishes. Two days later, cells were treated with indicated drug at the IC_{50} for 72 h then harvested and stained for Annexin V using FITC Annexin V Apoptosis Dectection kit (BD Pharmingen) according to the manufacturer's instruction. Stained samples were analyzed using FACS Calibur 1.

Microarray Gene Expression Analysis. RNAs were labeled and hybridized to Illumina expression arrays according to the manufacturer's protocol (http://www.illumina.com). Illumina HumanHT-12 V4 chips were used. All genes on the arrays were verified by BLAST and annotated using recent versions of public NCBI databases. Microarray analysis was performed using BeadStudio 3 and in-house Visual Basic software MATRIX 1.5. Array data were quantile-normalized and compared by calculating $\log_2$ ratios for each gene along with a t test p-value. The complete data has been deposited at GEO and is presented in Supplementary Data 1.

Chromatin Immunoprecipitations in HCC407 Cells. ChIP experiments were carried out using the Millipore ChIP Assay Kit (Millipore, no. 17-295) according to the manufacturer's instructions with the modifications outlined in Supporting Information. Primers used to scan the promoter and into the coding region are listed in Supporting Information.

Western Blot Analysis. Histones were extracted according to Shechter et al.[37] with the following modification. One million LDR cells were plated on 100 mm dishes. The next day, cells were treated with TSA (14 nM), **5** (1.5 μM), or DMSO for 24 h. Cells were harvested and processed according to ref 37. Histone extracts were separated on 4−12% NuPAGE Bis-Tris gels (Life Technologies). Histones were detected using anti-acetyl-histone H3 (Upstate), histone H3K4 trimethyl (Millipore), histone H3K9 trimethyl (Millipore), and total histone H3 (Active Motif) according to the manufacturer's instructions.

■ ASSOCIATED CONTENT

Ⓢ Supporting Information

This material is available free of charge via the Internet at http://pubs.acs.org.

Accession Codes

Microarray data has been deposited at GEO, accession code GSE59077. Assay results have been deposited in PubChem AID 1653.

■ AUTHOR INFORMATION

Corresponding Author

*E-mail: elisabeth.martinez@utsouthwestern.edu.

Present Addresses

[#]Institute for Medical Radiation and Cell Research (MSZ) in the Center of Experimental Molecular Medicine (ZEMM), University of Würzburg, Würzburg, Germany.

[⊥]Division of Cancer Biology, NCI, NIH, Rockville, MD.

Author Contributions

[+]These authors contributed equally to this work.

Notes

The authors declare no competing financial interest.

■ ACKNOWLEDGMENTS

This project was partly funded by the NCI (R01CA12526901 to E.D.M. and by the University of Texas SPORE in Lung Cancer P50-CA70907 to J.D.M., subaward to E.D.M.) and by the Doctor's Cancer Foundation (Nolan Miller Lung Cancer grant to E.D.M.). This research was supported in part by the Intramural Research Program of the NIH, National Cancer Institute, Center for Cancer Research. The authors would like to acknowledge the assistance of the Genomics Shared Resource at the Harold C. Simmons Cancer Center, which is supported in part by NCI Cancer Center Support Grant 1P30 CA142543-01. We also acknowledge the support of the NIH Roadmap for Medical Research. We are grateful to L. Girard for the use of Matrix and DIVISA software.

■ REFERENCES

(1) Doi, T., Hamaguchi, T., Shirao, K., Chin, K., Hatake, K., Noguchi, K., Otsuki, T., Mehta, A., and Ohtsu, A. (2012) Evaluation of safety, pharmacokinetics, and efficacy of vorinostat, a histone deacetylase inhibitor, in the treatment of gastrointestinal (GI) cancer in a phase I clinical trial. *Int. J. Clin. Oncol. 18*, 87−95.

(2) Hajek, R., Siegel, D., Orlowski, R. Z., Ludwig, H., Palumbo, A., and Dimopoulos, M. A. (2013) The role of Hdac inhibitors in patients with relapsed/refractory multiple myeloma. *Leuk. Lymphoma 55*, 11−18.

(3) Ververis, K., Hiong, A., Karagiannis, T. C., and Licciardi, P. V. (2013) Histone deacetylase inhibitors (HDACIs): multitargeted anticancer agents. *Biologics 7*, 47−60.

(4) New, M., Olzscha, H., and La Thangue, N. B. (2012) HDAC inhibitor-based therapies: can we interpret the code? *Mol. Oncol. 6*, 637−656.

(5) Baylin, S. B., and Jones, P. A. (2011) A decade of exploring the cancer epigenome−biological and translational implications. *Nat. Rev. Cancer 11*, 726−734.

(6) Hassler, M. R., Klisaroska, A., Kollmann, K., Steiner, I., Bilban, M., Schiefer, A. I., Sexl, V., and Egger, G. (2012) Antineoplastic activity of the DNA methyltransferase inhibitor 5-aza-2'-deoxycytidine in anaplastic large cell lymphoma. *Biochimie 94*, 2297−2307.

(7) Duvic, M., and Vu, J. (2007) Vorinostat: a new oral histone deacetylase inhibitor approved for cutaneous T-cell lymphoma. *Expert Opin. Investig. Drugs 16*, 1111−1120.

(8) Nebbioso, A., Carafa, V., Benedetti, R., and Altucci, L. (2012) Trials with 'epigenetic' drugs: an update. *Mol. Oncol. 6*, 657−682.

(9) Filippakopoulos, P., Qi, J., Picaud, S., Shen, Y., Smith, W. B., Fedorov, O., Morse, E. M., Keates, T., Hickman, T. T., Felletar, I., Philpott, M., Munro, S., McKeown, M. R., Wang, Y., Christie, A. L., West, N., Cameron, M. J., Schwartz, B., Heightman, T. D., La Thangue, N., French, C. A., Wiest, O., Kung, A. L., Knapp, S., and Bradner, J. E. (2010) Selective inhibition of BET bromodomains. *Nature 468*, 1067−1073.

(10) Tan, J., Yang, X., Zhuang, L., Jiang, X., Chen, W., Lee, P. L., Karuturi, R. K., Tan, P. B., Liu, E. T., and Yu, Q. (2007) Pharmacologic disruption of Polycomb-repressive complex 2-mediated gene repression selectively induces apoptosis in cancer cells. *Genes Dev. 21*, 1050−1063.

(11) Kruidenier, L., Chung, C. W., Cheng, Z., Liddle, J., Che, K., Joberty, G., Bantscheff, M., Bountra, C., Bridges, A., Diallo, H., Eberhard, D., Hutchinson, S., Jones, E., Katso, R., Leveridge, M., Mander, P. K., Mosley, J., Ramirez-Molina, C., Rowland, P., Schofield, C. J., Sheppard, R. J., Smith, J. E., Swales, C., Tanner, R., Thomas, P., Tumber, A., Drewes, G., Oppermann, U., Patel, D. J., Lee, K., and Wilson, D. M. (2012) A selective jumonji H3K27 demethylase inhibitor modulates the proinflammatory macrophage response. *Nature 488*, 404−408.

(12) Sayegh, J., Cao, J., Zou, M. R., Morales, A., Blair, L. P., Norcia, M., Hoyer, D., Tackett, A. J., Merkel, J. S., and Yan, Q. (2013) Identification of small molecule inhibitors of Jumonji AT-rich interactive domain 1B (JARID1B) histone demethylase by a sensitive high throughput screen. *J. Biol. Chem. 288*, 9408−9417.

(13) Kubicek, S., O'Sullivan, R. J., August, E. M., Hickey, E. R., Zhang, Q., Teodoro, M. L., Rea, S., Mechtler, K., Kowalski, J. A., Homon, C. A., Kelly, T. A., and Jenuwein, T. (2007) Reversal of H3K9me2 by a small-molecule inhibitor for the G9a histone methyltransferase. *Mol. Cell 25*, 473−481.

(14) Upadhyay, A. K., Rotili, D., Han, J. W., Hu, R., Chang, Y., Labella, D., Zhang, X., Yoon, Y. S., Mai, A., and Cheng, X. (2012) An analog of BIX-01294 selectively inhibits a family of histone H3 lysine 9 Jumonji demethylases. *J. Mol. Biol. 416*, 319−327.

(15) King, O. N., Li, X. S., Sakurai, M., Kawamura, A., Rose, N. R., Ng, S. S., Quinn, A. M., Rai, G., Mott, B. T., Beswick, P., Klose, R. J., Oppermann, U., Jadhav, A., Heightman, T. D., Maloney, D. J., Schofield, C. J., and Simeonov, A. (2010) Quantitative high-throughput screening identifies 8-hydroxyquinolines as cell-active histone demethylase inhibitors. *PLoS One 5*, e15535.

(16) Martinez, E. D., Dull, A. B., Beutler, J. A., and Hager, G. L. (2006) High-content fluorescence-based screening for epigenetic modulators. *Methods Enzymol. 414*, 21−36.

(17) Auld, D. S., Johnson, R. L., Zhang, Y. Q., Veith, H., Jadhav, A., Yasgar, A., Simeonov, A., Zheng, W., Martinez, E. D., Westwick, J. K., Austin, C. P., and Inglese, J. (2006) Fluorescent protein-based cellular assays analyzed by laser-scanning microplate cytometry in 1536-well plate format. *Methods Enzymol. 414*, 566−589.

(18) Johnson, R. L., Huang, W., Jadhav, A., Austin, C. P., Inglese, J., and Martinez, E. D. (2008) A quantitative high-throughput screen identifies potential epigenetic modulators of gene expression. *Anal. Biochem. 375*, 237−248.

(19) Best, A. M., Chang, J., Dull, A. B., Beutler, J. A., and Martinez, E. D. (2011) Identification of four potential epigenetic modulators from the NCI structural diversity library using a cell-based assay. *J. Biomed. Biotechnol. 2011*, 868095.

(20) Hsu, C. C., Li, H. P., Hung, Y. H., Leu, Y. W., Wu, W. H., Wang, F. S., Lee, K. D., Chang, P. J., Wu, C. S., Lu, Y. J., Huang, T. H., Chang, Y. S., and Hsiao, S. H. (2010) Targeted methylation of CMV and E1A viral promoters. *Biochem. Biophys. Res. Commun. 402*, 228−234.

(21) Duan, B., Cheng, L., Gao, Y., Yin, F. X., Su, G. H., Shen, Q. Y., Liu, K., Hu, X., Liu, X., and Li, G. P. (2012) Silencing of fat-1 transgene expression in sheep may result from hypermethylation of its driven cytomegalovirus (CMV) promoter. *Theriogenology 78*, 793−802.

(22) Michael, S., Auld, D., Klumpp, C., Jadhav, A., Zheng, W., Thorne, N., Austin, C. P., Inglese, J., and Simeonov, A. (2008) A robotic platform for quantitative high-throughput screening. *Assay Drug Dev. Technol. 6*, 637−657.

(23) Wang, Y., Jadhav, A., Southal, N., Huang, R., and Nguyen, D. T. (2010) A grid algorithm for high throughput fitting of dose-response curve data. *Curr. Chem. Genomics 4*, 57−66.

(24) Inglese, J., Auld, D. S., Jadhav, A., Johnson, R. L., Simeonov, A., Yasgar, A., Zheng, W., and Austin, C. P. (2006) Quantitative high-throughput screening: a titration-based approach that efficiently identifies biological activities in large chemical libraries. *Proc. Natl. Acad. Sci. U.S.A. 103*, 11473−11478.

(25) Simeonov, A., Jadhav, A., Sayed, A. A., Wang, Y., Nelson, M. E., Thomas, C. J., Inglese, J., Williams, D. L., and Austin, C. P. (2008) Quantitative high-throughput screen identifies inhibitors of the Schistosoma mansoni redox cascade. *PLoS Neglected Trop. Dis. 2*, e127.

(26) Wang, L., Chang, J., Varghese, D., Dellinger, M., Kumar, S., Best, A. M., Ruiz, J., Bruick, R., Pena-Llopis, S., Xu, J., Babinski, D. J., Frantz, D. E., Brekken, R. A., Quinn, A. M., Simeonov, A., Easmon, J., and Martinez, E. D. (2013) A small molecule modulates Jumonji histone demethylase activity and selectively inhibits cancer growth. *Nat. Commun. 4*, 2035.

(27) Shimamura, T., Chen, Z., Soucheray, M., Carretero, J., Kikuchi, E., Tchaicha, J. H., Gao, Y., Cheng, K. A., Cohoon, T. J., Qi, J., Akbay,

E., Kimmelman, A. C., Kung, A. L., Bradner, J. E., and Wong, K. K. (2013) Efficacy of BET bromodomain inhibition in Kras-mutant non-small cell lung cancer. *Clin. Cancer Res. 19*, 6183−6192.
(28) Herrmann, H., Blatt, K., Shi, J., Gleixner, K. V., Cerny-Reiterer, S., Mullauer, L., Vakoc, C. R., Sperr, W. R., Horny, H. P., Bradner, J. E., Zuber, J., and Valent, P. (2012) Small-molecule inhibition of BRD4 as a new potent approach to eliminate leukemic stem- and progenitor cells in acute myeloid leukemia AML. *Oncotarget 3*, 1588−1599.
(29) Yang, Q., Lu, Z., Singh, D., and Raj, J. U. (2012) BIX-01294 treatment blocks cell proliferation, migration and contractility in ovine foetal pulmonary arterial smooth muscle cells. *Cell Proliferation 45*, 335−344.
(30) Schenone, M., Dancik, V., Wagner, B. K., and Clemons, P. A. (2013) Target identification and mechanism of action in chemical biology and drug discovery. *Nat. Chem. Biol. 9*, 232−240.
(31) Martinez Molina, D., Jafari, R., Ignatushchenko, M., Seki, T., Larsson, E. A., Dan, C., Sreekumar, L., Cao, Y., and Nordlund, P. (2013) Monitoring drug target engagement in cells and tissues using the cellular thermal shift assay. *Science 341*, 84−87.
(32) Martinez, E. D., Rayasam, G. V., Dull, A. B., Walker, D. A., and Hager, G. L. (2005) An estrogen receptor chimera senses ligands by nuclear translocation. *J. Steroid Biochem. Mol. Biol. 97*, 307−321.
(33) Ramirez, R. D., Sheridan, S., Girard, L., Sato, M., Kim, Y., Pollack, J., Peyton, M., Zou, Y., Kurie, J. M., Dimaio, J. M., Milchgrub, S., Smith, A. L., Souza, R. F., Gilbey, L., Zhang, X., Gandia, K., Vaughan, M. B., Wright, W. E., Gazdar, A. F., Shay, J. W., and Minna, J. D. (2004) Immortalization of human bronchial epithelial cells in the absence of viral oncoproteins. *Cancer Res. 64*, 9027−9034.
(34) Bowen, W. P., and Wylie, P. G. (2006) Application of laser-scanning fluorescence microplate cytometry in high content screening. *Assay Drug Dev. Technol. 4*, 209−221.
(35) Southall NT, J. A., Huang, R, Nguyen, T, Wang, Y. (2009) Enabling the large scale analysis of quantitative high throughput screening data, in *Handbook of Drug Screening* (Seethala, R. and Zhang, L., Eds.), pp 442−463, Taylor and Francis, New York.
(36) Bookout, A. L., Cummins, C. L., Mangelsdorf, D. J., Pesola, J. M., and Kramer, M. F. (2006) High-throughput real-time quantitative reverse transcription PCR. *Curr. Protoc. Mol. Biol.*, DOI: 10.1002/0471142727.mb1508s73.
(37) Shechter, D., Dormann, H. L., Allis, C. D., and Hake, S. B. (2007) Extraction, purification and analysis of histones. *Nat. Protoc. 2*, 1445−1457.